

Chapter 4

Photochemical Smog in Southern China: a Synthesis of Observations and Model Investigations of the Sources and Effects of Nitrous Acid

Tao Wang¹, Yutong Liang¹, Qiaozhi Zha^{1,2}, Li Zhang¹, Zhe Wang¹, Weihao Wang¹, Steven Poon¹

Abstract Recent studies have revealed potentially important effects of additional source(s) of hydroxyl radicals on the atmosphere's oxidative capacity and, in turn, the production of secondary air pollutants. In this paper, we give an overview of our recent efforts in investigating the sources and effects of nitrous acid (HONO) on ozone and some secondary aerosols in southern China by combining field measurements and model simulations. Beginning in 2011, a series of field measurements of HONO were conducted at five sites, with diverse land use and different effects of emission sources. We observed the seasonal characteristics, emission ratios, heterogeneous production, and simulations of a chemical transport model for the photochemical effects of HONO. The key findings are as follows. The derived emission ratios from vehicles exhibited wide variability and were mostly higher than the more uniform value of 0.8% reported in the literature. Larger nocturnal heterogeneous conversion rates of NO₂ to HONO were observed when air masses were passing over sea surfaces, compared with land surfaces. Widely reported daytime sources of HONO also exist in Hong Kong. Moreover, the revised WRF-Chem model with comprehensive HONO sources significantly improved the simulations of the observed HONO, which enhanced regional hydroxyl radicals, O₃, and PM_{2.5} by 10-20, 8-15, and 10-15% over urban areas in the Pearl River Delta region, respectively. Our studies highlight the importance of considering HONO sources when simulating secondary pollutants in polluted atmospheres.

Keywords Nitrous acid (HONO), field measurement, WRF-Chem, secondary pollutants

4.1 Introduction

Air pollution is a serious problem in many Chinese urban areas. The frequent outbreaks of extremely heavy haze in Beijing attract major attention from the media, citizens, and regulatory agencies. This then prompts the central government to revise air-quality standards and launch stringent control measures in China's three most developed urban clusters. Previous research and control efforts have focused on particulate matter, which is

¹Department of Civil and Environmental Engineering at the Hong Kong Polytechnic University, Kowloon, Hong Kong, China

Email: cetwang@polyu.edu.hk

²Department of Physics, University of Helsinki, Helsinki, Finland

most severe in the winter, but processes affecting photochemical pollutants such as ozone and other secondary pollutants have not been comprehensively examined. One emerging issue is the effects of new radical(s) such as chlorine (e.g., Osthoff et al., 2008), or additional source(s) of hydroxyl radicals (Kleffmann, 2007) on the atmosphere's oxidative capacity and, subsequently, the production of secondary air pollutants such as ozone and some aerosol constituents. Studies conducted worldwide in the last ten years have confirmed that HONO can play an important role in the chemistry of a polluted atmosphere, not only in the morning, but also throughout the day. However, the sources of HONO in different environments and its effect on secondary pollutants in China are not well understood.

HONO in the atmosphere comes from a wide range of sources. Direct emissions include the release of HONO from fossil fuel combustion (e.g., Kurtenbach et al., 2001) and the microbial activities in soil (Su et al., 2011). The chemical formation of HONO includes gas-phase reactions of $\text{NO} + \text{OH}$ and heterogeneous processes on surfaces, such as the redox reaction of nitrogen dioxide (NO_2) on Black Carbon (BC) and semi-volatile species (e.g., Ammann et al., 1998), and the conversion of NO_2 to HONO on wet surfaces—the latter of which is often the dominant source of nocturnal HONO (Kleffmann, 2007).

One topic under intense research is the sources/processes contributing to elevated levels of daytime HONO, which cannot be explained by the homogenous reaction between NO and OH and the sources just mentioned (Acker and Möller, 2007, Czader et al., 2012, Czader et al., 2013, Li et al., 2012, Qin et al., 2009, Sörgel et al., 2011, Su et al., 2008, VandenBoer et al., 2014). Several possible photo-enhanced sources have been proposed, including the light-dependent heterogeneous reactions of NO_2 with aerosol and ground surfaces, the photolysis of HNO_3 absorbed on surfaces, the reaction of excited NO_2 with water vapors, and the reaction of NO_2 with $\text{HO}_2 \cdot \text{H}_2\text{O}$ (Kleffmann, 2007, Monge et al., 2010, Li et al., 2008, Li et al., 2014, Wong et al., 2011, Zhou et al., 2011).

Current state-of-the-art photochemical models treat the various HONO sources with potentially large uncertainties. The HONO/ NO_x emission ratios have only been measured in limited locations. The exact mechanisms of non-gaseous HONO pathways remain unclear, and parameterizations of these sources in the models are highly simplified, with large variations in the key parameters (e.g., the uptake coefficient of NO_2 on surfaces (γ_{NO_2}) varying from 10^{-6} to 10^{-4}) in different modeling studies. This has led to different conclusions on the importance of atmospheric aerosols in HONO formation (An et al., 2013, Li et al., 2010, Li et al., 2011, Sarwar et al., 2008, Aumont et al., 2003). In addition, emissions from soil microbial processes and the conversion of NO_2 on the ocean surface have not been considered in most of the previous model studies.

In this paper, we provide an overview of our recent efforts in investigating the sources and effects of HONO on ozone and some secondary aerosols in southern China by combining field measurements and modeling simulations. Due to their sub-tropic location, Hong Kong and the part of the Pearl River Delta in Guangdong Province on China's mainland have long suffered year-round photochemical pollution (e.g., Wang et al., 2001, Xue et al., 2014). Since 2011, a series of field studies on HONO have been conducted in five Hong Kong locations: a tunnel, a roadside site, a suburban area, a coastal area, and a mountain top (974 m a.s.l.). The data represent a wide range of conditions, from the source to the background, and from the surface to the top of the Planetary Boundary Layer (PBL). This paper provides an overview of the main characteristics of this dataset and synthesizes the key findings from

the analysis, including seasonal characteristics, emission ratios, heterogeneous production, and model simulations of photochemical effects.

4.2 Measurement Sites and Instrumentation

4.2.1 Measurement Sites

The locations of the five measurement sites are shown in Figure 4.1. The times the measurements were taken and the mean, maximum, and minimum concentrations of HONO are listed in Table 4.1. The Shing Mun Tunnel (SMT) site, located deep inside the north bore of the SMT (1.6 km in length), hosts 25,910 vehicles (over 40% diesel) per day, on average. The Mong Kok (MK) site, with a sampling point of less than 5 m from traffic and 2 m a.g.l., is situated at the junction of two major roads in Kowloon. The Tung Chung (TC) site (16 m a.g.l.) is in a newly developed residential area 3 km south of Hong Kong International Airport. This site is 80 m south of the North Lantau Highway, which is the only road connecting the airport and Tung Chung New Town with the city center. The Hok Tsui (HT) site is located in a relatively remote coastal area 10 km southeast of downtown Hong Kong Island, and does not feature any strong emission sources close by. The mountain-top Tai Mao Shan (TMS) site sits on Tai Mo Shan, the highest point in Hong Kong. The altitude (974 m a.s.l.) is slightly beneath the average height of the PBL, which varies between 1.2 km (autumn) and 1.0 km (winter) (Yang et al., 2013).

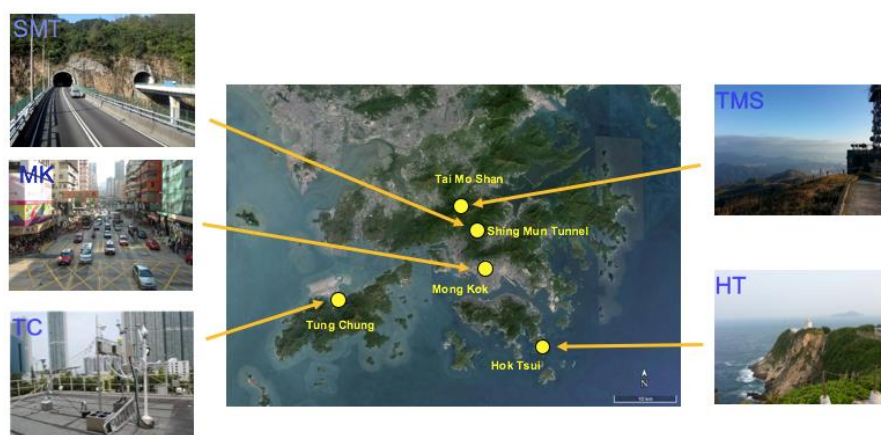


Fig. 4.1 Locations and views of the five Hong Kong measurement sites used in this study

Tab. 4.1 Site information with mean and range of concentrations

Site Reference	Time	Description	Mean NO_x (ppb)	Mean HONO (ppb)	Range of HONO (ppb)
Shing Mun Tunnel (SMT)	Mar 11-21, 2015	Tunnel with dense traffic	1117.3	15.79	7.78-30.67
Mong Kok (MK)	Mar 28-May 4, 2015	Roadside	129.0	3.26	0.12-15.44
Tung Chung (TC)	Aug and Nov 2011 Feb and May 2012	Suburban	23.2	0.71	BDL-5.00
Hok Tsui (HT)	Sep 1-Dec 19, 2012	Coastal	5.48	0.16	BDL-1.15
Tai Mo Shan (TMS)	Nov 15-Dec 6, 2013	Mountain-top	3.24	0.14	BDL-0.58

BDL: Below Detection Limit

4.2.2 Instrumentation

The HONO was measured with a commercial Long Path Absorption Photometer (QUMA, Model LOPAP-03) (Heland et al., 2001). The ambient air was sampled using two temperature-controlled stripping coils in series with a mixture reagent of 100 g sulfanilamide and 1 L HCl (37% v/v) in 9 L of pure water. In the first stripping coil, most of the HONO and a fraction of interfering substances were absorbed in solution R1. In the second stripping coil, the remaining HONO and most of the interfering species were absorbed in solution R2. After adding a reagent of 1.6 g N-naphtylethylenediamine-dihydrochloride in 9 L of pure water to both coils, colored azo dye was formed in solutions R1 and R2, which were then separately detected via long path absorption in special Teflon tubing. The HONO signal was the difference between the signals in the two channels. Compressed air was injected into the instrument to correct for the small drifts in baseline, and a span check was conducted to check the sensitivity of the instrument. Before each campaign, an HONO-source generator (QUMA, Model QS-03) was used to determine the sampling efficiency of the HONO in the sampling unit, which was found to be 99.95%. For more details, the reader is referred to Xu et al. (2015).

4.3 Results and Discussion

4.3.1 Concentrations at the Four Ambient Sites

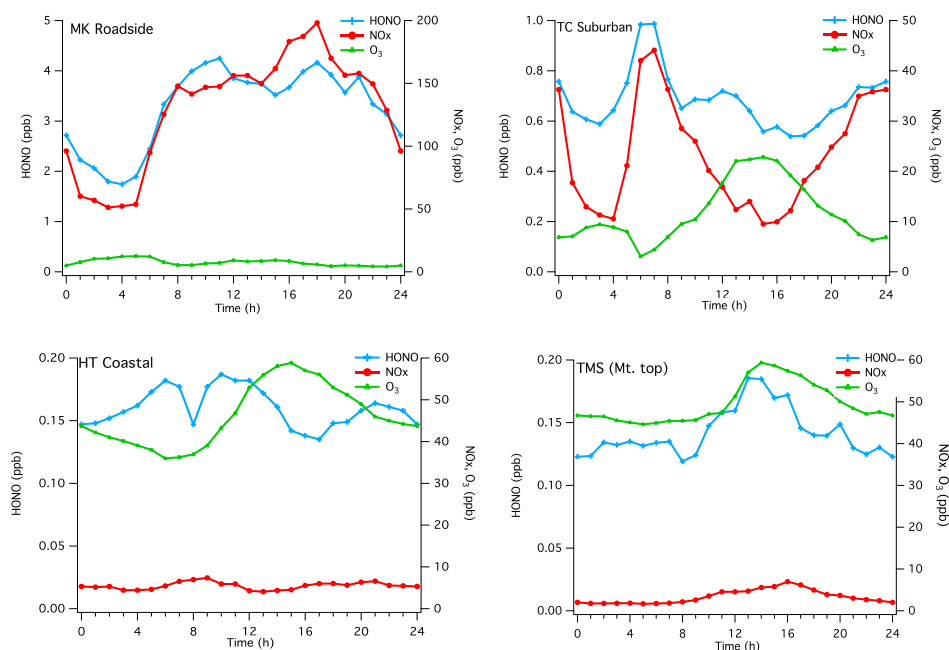


Fig. 4.2 Average mixing ratios of HONO, NO_x, and O₃ as a function of time of day at four ambient sites: MK (roadside), TC (suburban, August), HT (coastal background), and TMS (mountain top)

The concentrations of HONO revealed a cascade trend from the tunnel site (mean = 15.79 ppb), to the roadside site (3.26 ppb), to the suburban site (0.71 ppb), to the coastal site (0.16 ppb), to mountain-top background site (0.14 ppb) (Table 4.1). This result indicates that road traffic is an important source of HONO (either from direct emissions or from reaction(s) involving NO₂ emitted from vehicles). Diurnal patterns of HONO, NO_x, and O₃ at the four ambient sites are shown in Figure 4.2. The influence of vehicles was clearly seen in the roadside and suburban sites, as evidenced by the morning peaks (and afternoon rush hour at the roadside site). In contrast, the two remote sites showed HONO peaking at noon or in the early afternoon. At the TC site, HONO began to decline immediately after sunrise—a typical pattern in urban (Pusede et al., 2015, Lee et al., 2016, Wang et al., 2015), suburban (Tong et al., 2016, Michoud et al., 2014), and remote areas (Ren et al., 2010, Wojtal et al., 2011). However, this trend was not observed at the other three sites. The bimodal curve of HONO at MK can be attributed to the high traffic volume during rush hours, whereas the daytime peaks in HT and TMS can be explained by the heterogeneous conversion of NO₂ to HONO and variations in the height of the PBL, respectively.

At the TC site, HONO data were collected for one month in each of the four seasons. The highest concentration of HONO was found in late autumn (November), followed by late winter (February), late summer (August), and late spring (May). The mean HONO mixing ratios for these four seasons were 0.93 ± 0.78 , 0.91 ± 0.74 , 0.66 ± 0.53 , and 0.35 ± 0.30 ppb, respectively. The seasonal profiles of the HONO were similar to those of the other gases, such as CO and NO_x.

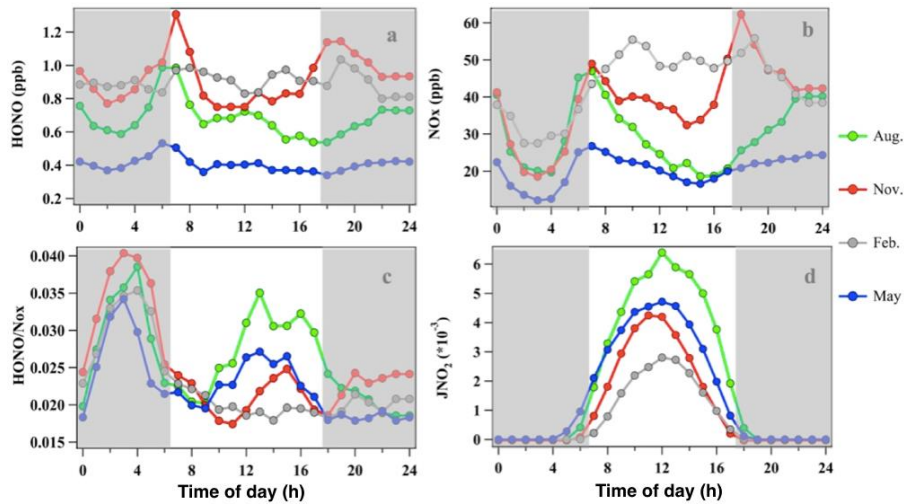


Fig. 4.3 Diurnal variations of (a) HONO, (b) NO_x, (c) HONO/NO_x, and (d) JNO₂ in February, May, August, and November at the TC sites. The gray shading refers to the nighttime period (18:00–06:00). Figure adapted from Xu et al. (2015)

The mean concentration of HONO at the MK roadside site was more than four times larger than that measured at a roadside site in Houston (Rappenglück et al., 2013), while the averaged HONO/NO_x ratio was only 12% larger. The mixing ratios of HONO and NO_x at our urban-influenced coastal background site (HT) were much higher, compared with those observed within the Marine Boundary Layer (MBL) of the Atlantic Ocean near North Carolina (Ye et al., 2016). HONO and NO₂ at our TMS site exhibited similar levels and trends to those measured on a rural mountain in Germany (Acker et al., 2006), although the noon peak of HONO in our measurement was much sharper. This may have been related to an upward transport of polluted air mass from the urban area to the hilltop once the PBL was broken up.

4.3.2 Emission Ratio from Road Traffic

The emission ratios of HONO/NO_x can be derived from measurements taken in the tunnel and in fresh plumes at a receptor site. Figure 4.4 shows a moderately positive correlation between HONO and NO_x (10-minute data) during the high-traffic period (7:00–22:00) inside the SMT. The emission ratio (HONO/NO_x) was highly variable, but the majority of the data points fell between the [HONO] = 0.6% [NO_x] and [HONO] = 2.3% [NO_x] lines, which is in line with the measurements taken in gasoline vehicle-dominated tunnels (Kirchstetter et al., 1996, Kurtenbach et al., 2001), and the upper limit of HONO/NO_x obtained in a lab study with diesel exhausts (Gutzwiller et al., 2002).

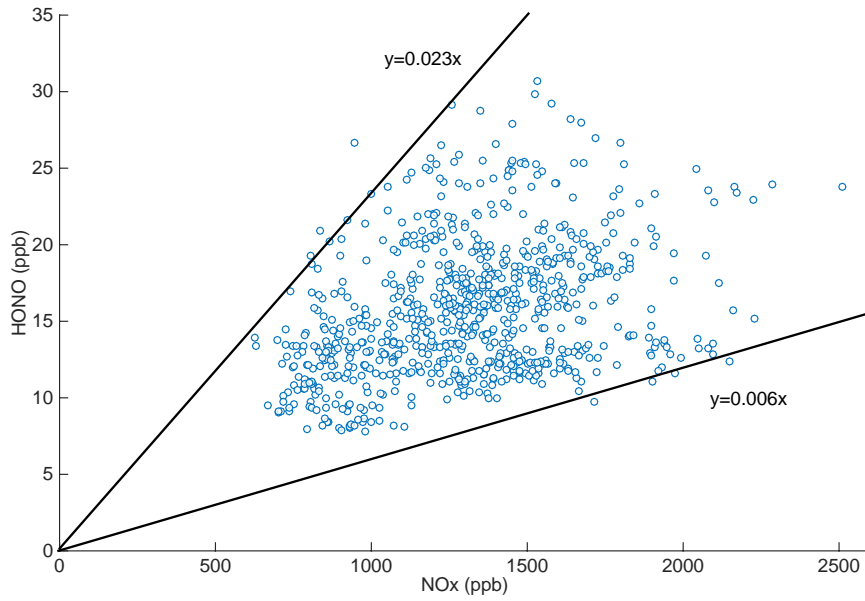


Fig. 4.4 Scatter plot of 10-min averaged HONO vs. NO_x in the Shing Mun Tunnel

At the TC suburban site, 21 freshly emitted plumes in the dark were selected based on the sharp increase in NO compared with NO₂, and the good correlation between HONO and NO_x (Xu et al., 2015). The derived emission ratios $\Delta[\text{HONO}]/\Delta[\text{NO}_x]$ from vehicular plumes were mostly higher than the commonly adopted value of 0.8% (Kurtenbach et al., 2001), and were found to be positively and almost linearly related to the emission of BC (Figure 4.5). This result suggests that BC seems to enhance the formation of HONO in fresh emissions, and this process (i.e., the heterogeneous reduction of NO₂ on fresh BC) must be considered in modeling studies, especially in locations that are close to road traffic. An empirical formula— $\frac{\Delta\text{HONO}}{\Delta\text{NO}_x} = 0.0050 + 0.003\Delta\text{BC}$ (where ΔBC is in $\mu\text{g}/\text{m}^3$)—was proposed to account for this effect (Xu et al., 2015).

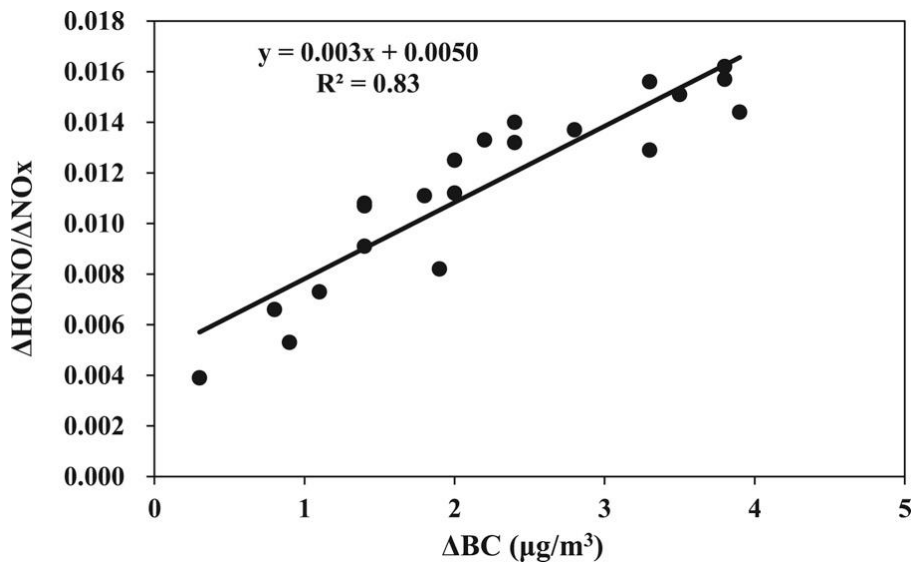


Fig. 4.5 Correlation of $\Delta\text{HONO}/\Delta\text{NO}_x$ with freshly emitted BC in the 21 fresh plumes. Figure adapted from Xu et al. (2015)

4.3.3 Derived Heterogeneous Production Rates of HONO

The heterogeneous production rates of HONO can be derived from ambient measurements of HONO and NO₂. At the coastal HT site, we selected six nighttime air masses in which the HONO concentration showed a steady increase while other gases such as ozone, CO, and NO_x were less variable, to rule out the photolytic reactions and the change in air mass (Figure 4.6). The conversion rates of NO₂ to HONO were calculated in these air masses using a slightly improved linear regression method based on the formula below (see Zha et al., 2014 for details).

$$C_{HONO} = \frac{[HONO](t_2) - [HONO](t_1)}{(t_2 - t_1) \times [\overline{NO_2}]}$$

where t_1 and t_2 are the starting and ending times of the case and $[\overline{NO_2}]$ is the average concentration of NO₂ during the period between t_1 and t_2 .

Six-hourly backward trajectories using the Hybrid Single-Particle Lagrangian Integrated Trajectory (HYSPLIT) model identified whether the air mass came over land or sea. Larger nocturnal heterogeneous conversion rates of NO₂ to HONO were observed when air masses passed over sea surfaces, than those passed over land surfaces (~3 times), suggesting that air-sea interactions may be a significant source of atmospheric HONO.

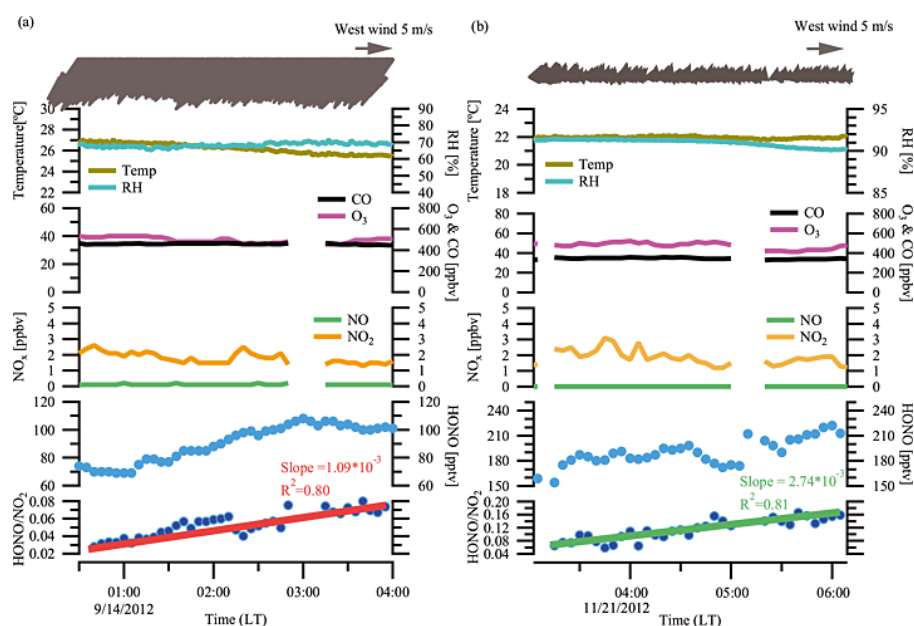


Fig. 4.6 (a) Land case from the night of September 13-14, 2012; (b) Sea case from the night of November 20-21, 2012. Figure adapted from Zha et al. (2014)

Figure 4.7 compares the NO₂ to HONO conversion rate in different atmospheric environments (Xu et al, 2015). The air masses that came over the sea at the HT site had the highest conversion rate, whereas the “land” case at the same site resembled those measured in other remote areas. The low conversion rate at the TC site could be due to nocturnal traffic emissions. The large variability in conversion rates suggests that air quality models should consider inhomogeneity of surface type when simulating NO₂ formation on ground/sea surfaces.

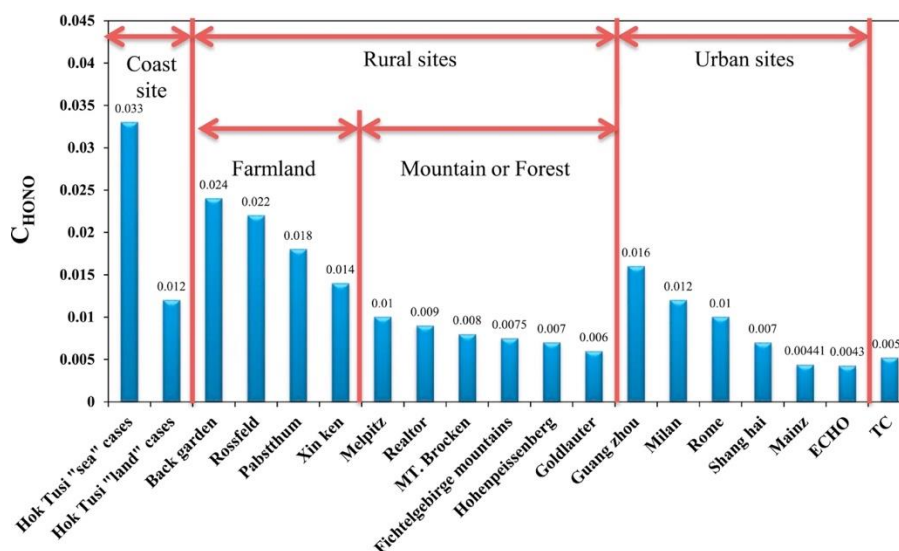


Fig. 4.7 Observed NO₂ to HONO conversion rates at HT, TC, and other sites. Figure adapted from Xu et al. (2015)

4.3.4 WRF-Chem Simulations on HONO Sources and Their Effects on Ozone and PM_{2.5}

We parameterized the up-to-date HONO sources into a widely used regional chemistry transport model (WRF-Chem). These sources included (1) heterogeneous reactions on ground surfaces, (2) photo-enhanced reactions on aerosol surfaces, (3) direct vehicle and vessel emissions, (4) potential conversion of NO₂ at the ocean surface, and (5) emissions from soil bacteria. Detailed parameterizations of the sources in the model can be found in Zhang et al. (2016). Seven simulation cases considering different HONO sources were designed in that study, as listed in Table 4.2.

Tab. 4.2 WRF-Chem Simulation cases considering different sources

Case	Additional HONO sources considered
BASE	Without additional HONO processes (i.e., with NO+OH only)
L	Heterogeneous sources from L and surfaces
LO	Heterogeneous sources from L and and O cean surfaces
LOA	Heterogeneous sources from L and, O cean, and A erosol surfaces
LOAE	Heterogeneous sources from L and, O cean, and A erosol surfaces and traffic Emissions
LOAES	Heterogeneous sources from L and, O cean, and A erosol surfaces, traffic Emissions and S oil emissions
LOAESG	Heterogeneous sources from L and, O cean, and A erosol surfaces, traffic Emissions and additional G as-phase formations

Figure 4.8 illustrates the mean observed and simulated HONO at the TC site in each case during August 20-31, 2011 when a multi-day photochemical episode occurred in the region. The heterogeneous conversion of NO₂ on the land surface was the dominant source (~42%) of the HONO observed at the TC site, followed by emissions from soil bacteria (23%), the oceanic source (9%), the gaseous formation via photochemical reaction consuming OH and NO (6%), and aerosol surfaces (3%). The results suggest that HONO sources in suburban areas could be more complex and diverse than those in urban or rural areas, indicating the need to consider the bacterial and ocean processes in HONO production in forested or coastal areas.

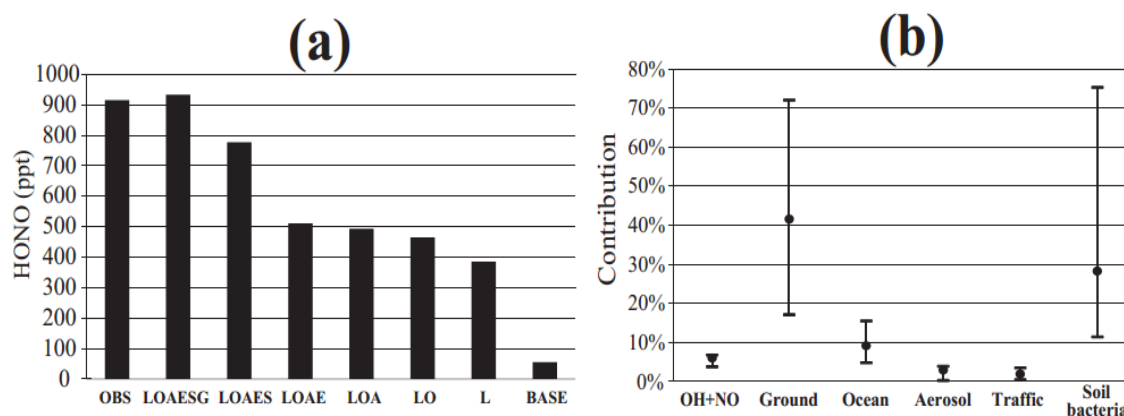


Fig. 4.8 (a) Averages of observed and simulated HONO and (b) contributions from homogeneous source (OH+NO), heterogeneous production on ground surface (Ground), oceanic source (Ocean), heterogeneous production on aerosol surface (Aerosol), traffic emissions (Traffic), and soil bacteria emissions (Soil bacteria) at the TC site. Figure adapted from Zhang et al (2016)

The inclusion of HONO sources has improved the WRF-Chem simulations of both daily and peak O₃ concentrations during noontime at multiple stations across Hong Kong (see Table 4.3). The mean biases between the simulated and observed values of 8- and 1-hour maxima O₃ in the LOAES case have appreciable improvements, decreasing from -10.03 ppb in the BASE case to -0.53 ppb, and from -21.77 ppb in the BASE case to -9.17 ppb, respectively. The daily average O₃ concentration at the measurement stations also increased from 30.34 ppb in the BASE case to 31.99 ppb in the LOAES case, much closer to the actual observations.

Tab. 4.3 Statistics of model performance in BASE and LOAES cases for hourly O₃, 8-hr maximum O₃, and 1-hr maximum O₃ at 12 air-quality monitoring stations in Hong Kong (unit: ppb)^a

	Metrics	OBS	BASE	LOAES
Hourly	Mean	30.97	30.34	31.99
	COR	/	0.75	0.78
	MB	/	-0.63	1.02
8-hr maximum	Mean	64.25	54.22	63.71
	COR	/	0.51	0.56
	MB	/	-10.03	-0.53
1-hr maximum	Mean	80.58	58.81	71.41
	COR	/	0.42	0.45
	MB	/	-21.77	-9.17

^aOBS: observation; Mean: averaged value; COR: correlation; MB: mean bias.

We further evaluated the effects on simulated O₃ and PM_{2.5} due to the considered heterogeneous sources of HONO. Figures 4.9 and 4.10 present the averaged distributions of modeled O₃ 14:00 LTC and daily PM_{2.5} in the BASE and LOAES cases over the PRD-HK region during August 25-31, 2011 (see Zhang et al., 2016 for details). As shown in Figure 4.8, high levels of O₃ of up to 80-100 ppb occurred over the northern parts of the PRD during the episode. Higher O₃ concentrations were shown over the downwind areas of the PRD in the LOAES case, especially over Hong Kong (Figure 4.10c), with an enhancement that reached up to 5-10 ppb (8-15%) over the urban areas in this region. The simulated PM_{2.5} was up to 80-90 µg/m³ in urban Guangzhou and Foshan and 50-60 µg/m³ in Shenzhen and Hong Kong in the BASE case. With inclusion of the additional HONO sources, the average PM_{2.5} increased to 60-70 µg/m³ in Shenzhen and Hong Kong. As shown in Figure 4.11c, the enhancements in total PM_{2.5} were around 8-10 µg/m³ (10-15%) in Guangzhou and Foshan, and 4-7 µg/m³ (5-15%) in Shenzhen, Dongguan, and Hong Kong. The increase in PM_{2.5} was mainly due to additional production of aerosol nitrate (see Figure 4.11). It is worth noting that the simulated effect of HONO on PM_{2.5} should be a lower limit of the actual effect because it is known that the current WRF-Chem model (and most other chemistry transport models) tends to under-simulate secondary organic aerosols. Thus, it is probable that the simulated increase in organic aerosols due to additional HONO sources may have been underestimated.

Overall, the incorporation of the aforementioned HONO into the model appreciably improved the ozone predictions at multiple monitoring stations in Hong Kong, and led to an 8-15% enhancement in averaged ozone and 10-15% in daily PM_{2.5} over the Pearl River Delta region and Hong Kong. Our results highlight the importance of accurately representing HONO sources in simulations of secondary pollutants over polluted regions.

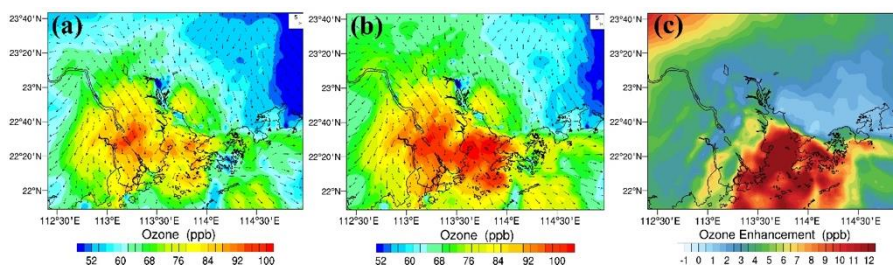


Fig. 4.9 Spatial distributions of simulated O₃ at 14:00 LTC over the PRD-HK in (a) BASE case and (b) LOAES case during the polluted period (August 25-31, 2011). Differences between BASE and LOAES cases are shown in (c)

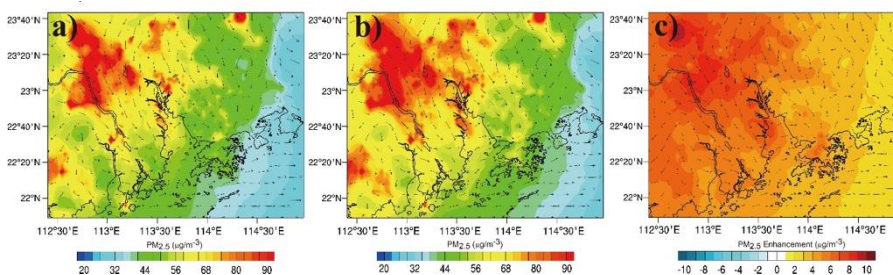


Fig. 4.10 Same as Fig. 4.9, but for daily PM_{2.5}

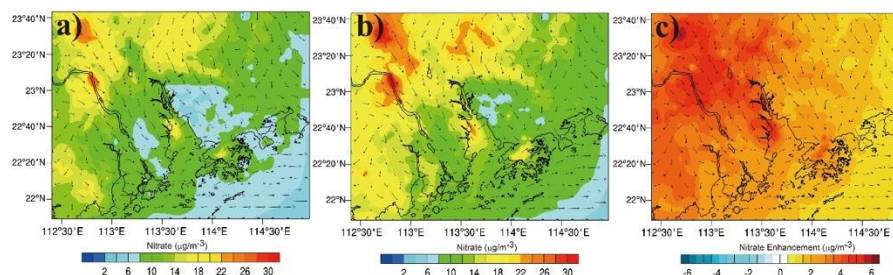


Fig. 4.11 Same as Fig. 4.9, but for daily PM_{2.5} nitrate

4.4 Concluding Remarks

As illustrated in our research in the Hong Kong region and others' findings, it is clear that HONO can be a very important source of hydroxyl radicals in polluted regions, which in turn play a critical role in atmospheric photochemistry and air pollution problems such as high ground-level ozone and haze. However, there are still significant uncertainties in quantifying HONO sources. Emissions from fuel combustion for various sources/under different conditions must be more fully understood, and soil emissions should be studied for a wide range of soil types and then properly represented in current models. The uptake processes of NO₂ on various surfaces (aerosol, terrestrial, and oceanic) should be better quantified, and our understanding of photo-related (daytime) sources could be improved. Emission-based air-quality models should consider the additional daytime sources of HONO (apart from reaction of OH and NO and vehicle emissions) in predicting secondary pollutants.

Acknowledgements The contributions to field measurements from Zheng Xu, Likun Xue, Shun Cheng Lee, Kin Fai Ho, Long Cui, Peter Louie, and Connie Luk are gratefully acknowledged. This work was supported by the Hong Kong Environmental Protection Department, Hong Kong Research Grants Council (C5022-14G), and Hong Kong Polytechnic University.

References

- Acker, K. & Möller, D. 2007. Atmospheric variation of nitrous acid at different sites in Europe. *Environmental Chemistry*, 4, 242-255.
- Acker, K., Moller, D., Wieprecht, W., Meixner, F. X., Bohn, B., Gilge, S., Plass-Dulmer, C. & Berresheim, H. 2006. Strong daytime production of OH from HNO₂ at a rural mountain site. *Geophysical Research Letters*, 33.
- Ammann, M., Kalberer, M., Jost, D. T., Tobler, L., Rossler, E., Piguet, D., Gaggeler, H. W. & Baltensperger, U. 1998. Heterogeneous production of nitrous acid on soot in polluted air masses. *Nature*, 395, 157-160.
- An, J., Li, Y., Chen, Y., Li, J., Qu, Y. & Tang, Y. 2013. Enhancements of major aerosol components due to additional HONO sources in the North China Plain and implications for visibility and haze. *Advances in Atmospheric Sciences*, 30, 57-66.
- Aumont, B., Chervier, F. & Laval, S. 2003. Contribution of HONO sources to the NO_x/HO_x/O₃ chemistry in the polluted boundary layer. *Atmospheric Environment*, 37, 487-498.
- Czader, B. H., Li, X. & Rappenglueck, B. 2013. CMAQ modeling and analysis of radicals, radical precursors, and chemical transformations. *Journal of Geophysical Research Atmospheres*, 118, 11376-11387.
- Czader, B. H., Rappenglück, B., Percell, P., Byun, D. W., Ngan, F. & Kim, S. 2012. Modeling nitrous acid and its impact on ozone and hydroxyl radical during the Texas Air Quality Study 2006. *Atmos. Chem. Phys.*, 12, 6939-6951.
- Gutzwiller, L., Arens, F., Baltensperger, U., Gaggeler, H. W. & Ammann, M. 2002. Significance of semivolatile diesel exhaust organics for secondary HONO formation. *Environmental Science & Technology*, 36, 677-682.
- Heland, J., Kleffmann, J., Kurtenbach, R. & Wiesen, P. 2001. A new instrument to measure gaseous nitrous acid (HONO) in the atmosphere. *Environmental Science & Technology*, 35, 3207-3212.
- Kirchstetter, T. W., Harley, R. A. & Littlejohn, D. 1996. Measurement of nitrous acid in motor vehicle exhaust. *Environmental Science & Technology*, 30, 2843-2849.
- Kleffmann, J. 2007. Daytime sources of nitrous acid (HONO) in the atmospheric boundary layer. *ChemPhysChem*, 8, 1137-1144.
- Kurtenbach, R., Becker, K. H., Gomes, J. a. G., Kleffmann, J., Lörzer, J. C., Spittler, M., Wiesen, P., Ackermann, R., Geyer, A. & Platt, U. 2001. Investigations of emissions and heterogeneous formation of HONO in a road traffic tunnel. *Atmospheric Environment*, 35, 3385-3394.
- Lee, J. D., Whalley, L. K., Heard, D. E., Stone, D., Dunmore, R. E., Hamilton, J. F., Young, D. E., Allan, J. D., Laufs, S. & Kleffmann, J. 2016. Detailed budget analysis of HONO in central London reveals a missing daytime source. *Atmos. Chem. Phys.*, 16, 2747-2764.
- Li, G., Lei, W., Zavala, M., Volkamer, R., Dusanter, S., Stevens, P. & Molina, L. T. 2010. Impacts of HONO sources on the photochemistry in Mexico City during the MCMA-2006/MILAGO Campaign. *Atmos. Chem. Phys.*, 10, 6551-6567.
- Li, S., Matthews, J. & Sinha, A. 2008. Atmospheric hydroxyl radical production from electronically excited NO₂ and H₂O. *Science*, 319, 1657-1660.
- Li, X., Brauers, T., Häsel, R., Bohn, B., Fuchs, H., Hofzumahaus, A., Holland, F., Lou, S., Lu, K. D., Rohrer, F., Hu, M., Zeng, L. M., Zhang, Y. H., Garland, R. M., Su, H., Nowak, A., Wiedensohler, A., Takegawa, N., Shao, M. & Wahner, A. 2012. Exploring the atmospheric chemistry of nitrous acid (HONO) at a rural site in Southern China. *Atmos. Chem. Phys.*, 12, 1497-1513.
- Li, X., Rohrer, F., Hofzumahaus, A., Brauers, T., Häsel, R., Bohn, B., Broch, S., Fuchs, H., Gomm, S., Holland, F., Jäger, J., Kaiser, J., Keutsch, F. N., Lohse, I., Lu, K., Tillmann, R., Wegener, R., Wolfe, G. M., Mentel, T. F., Kiendler-Scharr, A. & Wahner, A. 2014. Missing gas-phase source of HONO inferred from zeppelin measurements in the troposphere. *Science*, 344, 292-296.
- Li, Y., An, J., Min, M., Zhang, W., Wang, F. & Xie, P. 2011. Impacts of HONO sources on the air quality in Beijing, Tianjin and Hebei Province of China. *Atmospheric Environment*, 45, 4735-4744.
- Michoud, V., Colomb, A., Borbon, A., Miet, K., Beekmann, M., Camredon, M., Aumont, B., Perrier, S., Zapf, P., Siour, G., Ait-Helal, W., Afif, C., Kukui, A., Furger, M., Dupont, J. C., Haefelin, M. & Doussin, J.

- F. 2014. Study of the unknown HONO daytime source at a European suburban site during the MEGAPOLI summer and winter field campaigns. *Atmos. Chem. Phys.*, 14, 2805-2822.
- Monge, M. E., D'anna, B., Mazri, L., Giroir-Fendler, A., Ammann, M., Donaldson, D. J. & George, C. 2010. Light changes the atmospheric reactivity of soot. *Proceedings of the National Academy of Sciences*, 107, 6605-6609.
- Osthoff, H. D., Roberts, J. M., Ravishankara, A. R., Williams, E. J., Lerner, B. M., Sommariva, R., Bates, T. S., Coffman, D., Quinn, P. K., Dibb, J. E., Stark, H., Burkholder, J. B., Talukdar, R. K., Meagher, J., Fehsenfeld, F. C. & Brown, S. S. 2008. High levels of nitryl chloride in the polluted subtropical marine boundary layer. *Nature Geosci*, 1, 324-328.
- Pusede, S. E., Vandenboer, T. C., Murphy, J. G., Markovic, M. Z., Young, C. J., Veres, P. R., Roberts, J. M., Washenfelder, R. A., Brown, S. S., Ren, X., Tsai, C., Stutz, J., Brune, W. H., Browne, E. C., Wooldridge, P. J., Graham, A. R., Weber, R., Goldstein, A. H., Dusanter, S., Griffith, S. M., Stevens, P. S., Lefer, B. L. & Cohen, R. C. 2015. An atmospheric constraint on the NO₂ dependence of daytime near-surface nitrous acid (HONO). *Environmental Science & Technology*, 49, 12774-12781.
- Qin, M., Xie, P., Su, H., Gu, J., Peng, F., Li, S., Zeng, L., Liu, J., Liu, W. & Zhang, Y. 2009. An observational study of the HONO-NO₂ coupling at an urban site in Guangzhou City, South China. *Atmospheric Environment*, 43, 5731-5742.
- Rappenglück, B., Lubertino, G., Alvarez, S., Golovko, J., Czader, B. & Ackermann, L. 2013. Radical precursors and related species from traffic as observed and modeled at an urban highway junction. *Journal of the Air & Waste Management Association*, 63, 1270-1286.
- Ren, X., Gao, H., Zhou, X., Crouse, J. D., Wennberg, P. O., Browne, E. C., Lafranchi, B. W., Cohen, R. C., McKay, M., Goldstein, A. H. & Mao, J. 2010. Measurement of atmospheric nitrous acid at Bodgett Forest during BEARPEX2007. *Atmos. Chem. Phys.*, 10, 6283-6294.
- Sarwar, G., Roselle, S. J., Mathur, R., Appel, W., Dennis, R. L. & Vogel, B. 2008. A comparison of CMAQ HONO predictions with observations from the Northeast Oxidant and Particle Study. *Atmospheric Environment*, 42, 5760-5770.
- Sörgel, M., Regelin, E., Bozem, H., Diesch, J. M., Drewnick, F., Fischer, H., Harder, H., Held, A., Hosaynali-Beygi, Z., Martinez, M. & Zetzsch, C. 2011. Quantification of the unknown HONO daytime source and its relation to NO₂. *Atmos. Chem. Phys.*, 11, 10433-10447.
- Su, H., Cheng, Y., Oswald, R., Behrendt, T., Trebs, I., Meixner, F. X., Andreae, M. O., Cheng, P., Zhang, Y. & Pöschl, U. 2011. Soil nitrite as a source of atmospheric HONO and OH radicals. *Science*, 333, 1616-1618.
- Su, H., Cheng, Y. F., Shao, M., Gao, D. F., Yu, Z. Y., Zeng, L. M., Slanina, J., Zhang, Y. H. & Wiedensohler, A. 2008. Nitrous acid (HONO) and its daytime sources at a rural site during the 2004 PRIDE-PRD experiment in China. *Journal of Geophysical Research: Atmospheres*, 113, D14132.
- Tong, S., Hou, S., Zhang, Y., Chu, B., Liu, Y., He, H., Zhao, P. & Ge, M. 2016. Exploring the nitrous acid (HONO) formation mechanism in winter Beijing: direct emissions and heterogeneous production in urban and suburban areas. *Faraday Discussions*.
- Vandenboer, T. C., Markovic, M. Z., Sanders, J. E., Ren, X., Pusede, S. E., Browne, E. C., Cohen, R. C., Zhang, L., Thomas, J., Brune, W. H. & Murphy, J. G. 2014. Evidence for a nitrous acid (HONO) reservoir at the ground surface in Bakersfield, CA, during CalNex 2010. *Journal of Geophysical Research: Atmospheres*, 119, 9093-9106.
- Wang, L., Wen, L., Xu, C., Chen, J., Wang, X., Yang, L., Wang, W., Yang, X., Sui, X., Yao, L. & Zhang, Q. 2015. HONO and its potential source particulate nitrite at an urban site in North China during the cold season. *Science of The Total Environment*, 538, 93-101.
- Wang, T., Cheung, V. T. F., Anson, M. & Li, Y. S. 2001. Ozone and related gaseous pollutants in the boundary layer of eastern China: Overview of the recent measurements at a rural site. *Geophysical Research Letters*, 28, 2373-2376.
- Wojtal, P., Halla, J. D. & McLaren, R. 2011. Pseudo steady states of HONO measured in the nocturnal marine boundary layer: a conceptual model for HONO formation on aqueous surfaces. *Atmos. Chem. Phys.*, 11, 3243-3261.
- Wong, K. W., Oh, H. J., Lefer, B. L., Rappenglück, B. & Stutz, J. 2011. Vertical profiles of nitrous acid in the nocturnal urban atmosphere of Houston, TX. *Atmos. Chem. Phys.*, 11, 3595-3609.
- Xu, Z., Wang, T., Wu, J., Xue, L., Chan, J., Zha, Q., Zhou, S., Louie, P. K. K. & Luk, C. W. Y. 2015. Nitrous acid (HONO) in a polluted subtropical atmosphere: Seasonal variability, direct vehicle emissions and heterogeneous production at ground surface. *Atmospheric Environment*, 106, 100-109.
- Xue, L., Wang, T., Louie, P. K. K., Luk, C. W. Y., Blake, D. R. & Xu, Z. 2014. Increasing external effects negate local efforts to control ozone air pollution: A case study of Hong Kong and implications for other Chinese cities. *Environmental Science & Technology*, 48, 10769-10775.

- Yang, D., Li, C., Lau, A.K., & Li, Y. 2013. Long-term measurement of daytime atmospheric mixing layer height over Hong Kong. *Journal of Geophysical Research: Atmospheres* 118 (5):2422-2433. doi: 10.1002/jgrd.50251.
- Ye, C., Zhou, X., Pu, D., Stutz, J., Festa, J., Spolaor, M., Tsai, C., Cantrell, C., Mauldin, R. L., Campos, T., Weinheimer, A., Hornbrook, R. S., Apel, E. C., Guenther, A., Kaser, L., Yuan, B., Karl, T., Haggerty, J., Hall, S., Ullmann, K., Smith, J. N., Ortega, J. & Knote, C. 2016. Rapid cycling of reactive nitrogen in the marine boundary layer. *Nature*, 532, 489-491.
- Zha, Q., Xue, L., Wang, T., Xu, Z., Yeung, C., Louie, P. K. K. & Luk, C. W. Y. 2014. Large conversion rates of NO₂ to HNO₂ observed in air masses from the South China Sea: Evidence of strong production at sea surface? *Geophysical Research Letters*, 41, 7710-7715.
- Zhang, L., Wang, T., Zhang, Q., Zheng, J., Xu, Z. & Lv, M. 2016. Potential sources of nitrous acid (HONO) and their impacts on ozone: A WRF-Chem study in a polluted subtropical region. *Journal of Geophysical Research: Atmospheres*, 3645-3662.
- Zhou, X., Zhang, N., Teravest, M., Tang, D., Hou, J., Bertman, S., Alaghmand, M., Shepson, P. B., Carroll, M. A., Griffith, S., Dusanter, S. & Stevens, P. S. 2011. Nitric acid photolysis on forest canopy surface as a source for tropospheric nitrous acid. *Nature Geosci*, 4, 440-443.